1

Isotope tracing of submarine groundwater discharge offshore Ubatuba, Brazil: Results of the IAEA-UNESCO SGD project

P.P. Povinec[a,*], H. Bokuniewicz[b], W.C. Burnett[c], J. Cable[d], M. Charette[e],
J.-F. Comanducci[f], E.A. Kontar[g#], W.S. Moore[h], J.A. Oberdorfer[i],
J. de Oliveira[j], R. Peterson[c], T. Stieglitz[k], M. Taniguchi[l]

[a] *Comenius University, Faculty of Mathematics, Physics and Informatics, Bratislava, Slovakia*
[b] *Stony Brook University, Marine Sciences Research Center, Stony Brook, NY 11794-5000, USA*
[c] *Florida State University, Department of Oceanography, Tallahassee, FL 32306, USA*
[d] *Louisiana State University, Department of Oceanography and Coastal Science, Baton Rouge, LA 70803;USA*
[e] *Woods Hole Oceanographic Institution, Woods Hole, MA 02543, USA,*
[f] *International Atomic Energy Agency, Marine Environment Laboratories, Monaco*
[g] *Shirshov Institute of Oceanology, Moscow, Russian Federation*
[h] *University of South Carolina, Department of Geological Sciences, Columbia, SC 20208, USA*
[i] *San Jose State University, Department of Geology, San Jose, CA 95192-0102, USA*
[j] *Instituto de Pesquisas Energéticas e Nucleares, São Paulo, Brazil*
[k] *James Cook University, School of Mathematics, Physics and Information Technology, Townsville, Australia, and
Australian Institute of Marine Sciences, Townsville, Australia*
[l] *Research Institute for Humanity and Nature, Kyoto, Japan*

Abstract

Results of groundwater and seawater analyses for radioactive (^{3}H, ^{222}Rn, ^{223}Ra, ^{224}Ra, ^{226}Ra, ^{228}Ra) and stable (^{2}H, ^{18}O) isotopes are presented together with in situ spatial mapping and time-series ^{222}Rn measurements in seawater, direct seepage measurements using manual and automated seepage meters, pore water investigations using different tracers and piezometric techniques, and geoelectric surveys probing the coast. This study represents first time that such a new complex arsenal of radioactive and non-radioactive tracer techniques and geophysical methods have been used for simultaneous submarine groundwater discharge (SGD) investigations. Large fluctuations of SGD fluxes were observed at sites situated only a few meters apart (from 0 cm d^{-1} to 360 cm d^{-1}; the unit represents cm^3/cm^2/day), as well as during a few hours (from 0 cm d^{-1} to 110 cm d^{-1}), strongly depending on the tidal fluctuations. The average SGD flux estimated from continuous ^{222}Rn measurements is 17±10 cm d^{-1}. Integrated coastal SGD flux estimated for the Ubatuba coast using radium isotopes is about 7x10^3 m^3 d^{-1} per km of the coast. The isotopic composition (δ^2H and δ^{18}O) of submarine waters was characterised by significant variability and heavy isotope enrichment, indicating that the contribution of groundwater in submarine waters varied from a small percentage to 20%. However, this contribution with increasing offshore distance became negligible. Automated seepage meters and time-series measurements of ^{222}Rn activity concentration showed a negative correlation between the SGD rates and tidal stage. This is likely caused by sea level changes as tidal effects induce variations of hydraulic gradients. The geoelectric probing and piezometric measurements contributed to better understanding of the spatial distribution of different water masses present along the coast. The radium isotope data showed scattered distributions with offshore distance, which imply that seawater in a complex coast with many small bays and islands was influenced by local currents and groundwater/seawater mixing. This has also been confirmed by a relatively short residence time of 1-2 weeks for water within 25 km offshore, as obtained by short-lived radium isotopes. The irregular distribution of SGD seen at Ubatuba is a characteristic of fractured rock aquifers, fed by coastal groundwater and recirculated seawater with small admixtures of groundwater, which is of potential environmental concern and has implications on the management of freshwater resources in the region.

---

[*]Corresponding author. Experimental work was carried out during the author stay at the International Atomic Energy Agency, Marine Environment Laboratories, Monaco. Present address: Comenius University, Faculty of Mathematics, Physics and Informatics, Mlynska dolina F-1, SK-84248 Bratislava, Slovakia; Phone: +421 260 295 544; Fax: +421 265 425 882; E-mail address: **povinec@fmph.uniba.sk**
[#] Present address: Illinois State Geological Survey, Champaign, Illinois 61820-6964, USA

1. Introduction

Submarine groundwater discharge (SGD) is generally a widespread, but disperse coastal phenomenon that occurs wherever hydrogeologic gradients enable groundwater transport offshore. It has recently been shown to be a process of importance for management of freshwater resources and protection of coastal regions (Burnett et al., 2006). Most SGD occurs as a diffuse seepage, and identifying discharge sites or quantifying flux rates across the sediment-water interface has been difficult. Fluxes of SGD estimated from groundwater flow models are typically one to several orders of a magnitude smaller than those measured using field instruments or chemical tracers (Moore, 1996; Burnett et al., 2006). In addition, estimates of SGD depend strongly on the evaluation technique (Cable et al., 2004; Martin et al., 2004). Likewise, the source of water strongly influences the discharge measurement, as nearshore groundwater fluxes can be significantly different from offshore recirculated seawater through sediments (Martin et al., 2007). Benthic chambers, salinity and temperature measurements, chemical analyses, and measurements of a range of isotopic tracers at the aquifer-sea interface helped to estimate local and integrated coastal SGD fluxes (Burnett et al. 2006). Groundwater seepage is usually patchy, diffuse, temporally variable, and difficult to quantify. Specific methods have been developed for simulating seawater/freshwater interactions and seawater intrusion using salinity/temperature variations, tidal pumping, and wind and wave modelling. The most frequently used method for the estimation of SGD flux to the sea is based on seepage rate measurements (Bokuniewicz, 1992; Taniguchi et al., 2002); however, seawater circulation in coastal areas may not yield a realistic value for freshwater input into the sea via SGD (Burnett et al., 2001a).

Stable (^{2}H, ^{13}C, ^{15}N, ^{18}O), as well as radioactive (^{3}H, ^{14}C, Ra isotopes, radon) isotopes, have been applied to estimate integrated SGD fluxes over entire coasts as seepage measurements give information on SGD fluxes on local scales only (Cable et al., 1996; Moore, 2000; Burnett et al., 2001a, 2002, 2006; Kim & Hwang, 2002; Oliveira *et al.,* 2003; Moore & Wilson, 2005; Stieglitz, 2005; Moore, 2006; Povinec *et al*., 2006a; Weinstein *et al.,* 2006). An ideal SGD tracer should be highly enriched in groundwater relative to seawater, behave conservatively, and be easy measured. Deuterium and ^{18}O are useful conservative tracers of mixing processes at the groundwater-seawater interface, as they clearly distinguish between onshore meteoric groundwater and seawater (Povinec et al., 2008). Radium also fulfils the above mentioned conditions for a good SGD tracer. Four natural radium isotopes (^{223}Ra, $t_{1/2}$ = 11.4 d; ^{224}Ra, $t_{1/2}$ = 3.66 d; ^{226}Ra, $t_{1/2}$ = 1600 y and ^{228}Ra, $t_{1/2}$ = 5.75 y) have been used for the assessment of groundwater discharge, coastal water exchange rates in coastal zones, and for estimation of

residence time of water (Moore, 1996; Moore, 2000; Moore & Wilson, 2005; Moore, 2006; Moore & Oliveira, 2008). Short-lived radium isotopes are found in higher concentrations close to the continental margins. They are highly depleted in ocean basins due to their rapid decay and strong depletion in parent Th isotopes. One strong advantage of radium isotopes as SGD tracers is that the coastal water column effectively integrates the SGD signal over spatial and temporal scales. ^{222}Rn is also an ideal tracer for studying groundwater/seawater interactions since its concentration in groundwater is several orders of magnitude higher than in seawater. It is a direct decay product of ^{226}Ra from the ^{238}U natural radioactive chain, and due to short half-life (3.83 d), it is a suitable tracer for studying dynamic systems. Temporal and spatial monitoring of SGD has recently been possible due to new technologies that are based on the analysis of ^{222}Rn decay products emitting either alpha-rays (Burnett et al., 2001b; Burnett & Dulaiova, 2003, 2006) or gamma-rays (Povinec et al., 2001, 2006b).

This paper summarises the results obtained during the SGD intercomparison experiment carried out during November 14-26, 2003, along the Ubatuba coastal area in southeastern Brazil. The series of SGD investigations were carried out in the framework of the Coordinated Research Project (CRP) on ''Nuclear and Isotopic Techniques for the Characterisation of Submarine Groundwater Discharge in Coastal Zones'', which was organised from 2000 to 2005 by the International Atomic Energy Agency (IAEA), in cooperation with the United Nations Educational, Scientific and Cultural Organization (UNESCO). The project was coordinated by the IAEA's Isotope Hydrology Section in Vienna (P. Aggarwal and K. Kulkarni) and Marine Environment Laboratory in Monaco (P. Povinec), in cooperation with the UNESCO's Intergovernmental Oceanographic Commission (IOC) and International Hydrological Programme (IHP). Laboratories in Brazil, India, Italy, Japan, Russia, Turkey, Slovenia and USA took part in the CRP. The objectives of the CRP included the development of radioactive and non-radioactive tracer techniques. In addition to isotopic tracers, the group used automated seepage meters and electromagnetic geophysical surveys for the quantitative estimation of various components of SGD. Establishing more refined tools for assessing SGD contributed to better understanding the influence of SGD on coastal processes and on groundwater regimes, with implications on the management of water resources in coastal areas. Other joint IAEA-UNESCO SGD intercomparison exercises were carried out in Australia (2000), Sicily (2002), Long Island (2002) and Mauritius (2005). The aim was to test and to apply as many as possible tracer techniques for SGD investigations in different hydrogeologic environments, e.g. coastal plain (Australia), karst (Sicily), glaciofluvial deposits (Shelter Island), volcanic island (Mauritius), and fractured crystalline rocks (Brazil). The Ubatuba coastal area east of São Paulo was chosen for this pilot

project due to its granite geological structure, previous SGD investigations carried out by the IPEN (Instituto de Pesquisas Energéticas e Nucleares in São Paulo) and the University of São Paulo, and availability of logistical support. Previous work carried out at the Ubatuba site documented modest fluxes of SGD (Oliveira *et al*., 2003, 2006a, b). Contamination of bays with nutrients indicated their possible transport via groundwater, as well as by local currents (Povinec et al., 2008).

In this paper, we report the results of analysis of radioactive (^{3}H, ^{222}Rn, ^{223}Ra, ^{224}Ra, ^{226}Ra, ^{228}Ra) and stable (^{2}H, ^{18}O) isotopes in groundwater, seawater, and their mixtures. In addition, in situ spatial mapping and time-series ^{222}Rn measurements in seawater, direct seepage measurements using manual and automated seepage meters with continuous monitoring of temperature and salinity, pore water investigations using different tracers, geoelectric surveys, and development of a hydrogeologic model were carried out. All of these very different techniques were applied to assess SGD at the same site and time. This represents the first time that such a complex arsenal of radioactive and non-radioactive tracer techniques have been used for simultaneous SGD investigations. This paper is a continuation in the series of papers on the development of nuclear and isotopic technologies for SGD quantification (Povinec et al., 2006a).

2. Hydrogeology and coastal oceanography of the region

A quantification of SGD in a fractured-rock aquifer environment is a difficult task due to the spatial variability in aquifer properties resulting from the variability in the spacing, aperture, and interconnectedness of the fractures. The study area is located in the Pre-Cambrian shield region of eastern Brazil (**Fig. 1**). Groundwater occurs in fractures in the granitic and metamorphic rocks of the area, and not a great deal is known about the groundwater in the fractured bedrock since it is not used to a significant degree as a resource. There is some utilization of localized springs related to major fractures. The region is one of the highest rainfall regions of Brazil, which means recharge is likely to occur readily.

The intercomparison experiment was carried out in a series of small embayments near the city of Ubatuba, São Paulo State (Fig. 1). The embayments included Flamengo Bay (where there is an Oceanography Base run by the University of São Paulo that served as a base of operations), Fortaleza Bay, Mar Virado Bay, Ubatuba Bay, and Picinguaba Bay. The geological, geomorphologic, and hydrogeological characteristics of the area are strongly controlled by the presence of fractured crystalline rocks, especially the granites and migmatites of a mountain chain called Serra do Mar (altitudes up to 1,000 meters), which reaches the shore throughout most

of the study area, and limits the extension of the drainage systems and of the Quaternary coastal plains (Mahiques, 1995). The mean annual rainfall is about 1,800 mm, and the maximum rainfall rates usually occur in February. The rain-runoff regime due to the humid tropical climate and the absence of large river basins in the area is important for the transport of freshwater from the continent to the ocean. Despite the small drainage basins between the mountain range and the shore, freshwater discharge is sufficient to reduce the salinity of coastal waters.

Three water masses occur in the area: (i) Coastal Water (CW), characterized by high temperatures (>25°C) and low salinity (32-33); (ii) Tropical Water (TW), with intermediate temperatures (20-23°C) and high salinity (~36); and (iii) South Atlantic Central Water (SACW), with low temperatures (16-18°C) and high salinity (35-36). During the summer, nutrient-rich SACW moves onshore and is often found in the central and outer portions of the continental shelf (20-100 m water depth), while CW is found along a narrow band inshore. These water movements result in a vertical stratification over the inner shelf, with a strong thermocline at middle depths. In the winter (May through August), when SACW is restricted to the outer shelf, horizontal and vertical thermal gradients are reduced and almost no stratification is observed on the inner shelf (Castro Filho *et. al.*, 1987). In the summer, the advance of the SACW over the coast leads to the displacement of the CW, which is rich in continental suspended materials. In the winter, the retreat of the SACW and the decrease of rain levels restrict the input of sediments from continental areas. In Flamengo Bay, the tidal range is between 4.4 and 5.5 m, and the highest (4.4 – 5.9 m) is observed in August-September due to a greater volume of warm waters of the Brazil Current (Mesquita, 1997). Wave action is the most effective hydrodynamic phenomenon responsible for the bottom sedimentary processes in the coastal area, as well as in the adjacent inner continental shelf.

The beach at the Flamengo Bay was selected for in-depth studies because of the presence of weathered bedrock and sediment above the fractured granite. This granular material permitted the installation of wells and equipment that would not have been possible to install in fresh, fractured bedrock. Understanding SGD on this small scale should provide insight into data collected on a much larger scale and targeted by geochemical tracer studies carried out at the same time.

3. Methods

3.1. Field measurements

Conductivity/resistivity investigations were carried out to reveal the structure of the flow field of the freshwater component of SGD, as described in detail by Stieglitz et al. (2008). The electrical properties of the beach sediments were investigated with *in situ* conductivity sensors inserted into the sediment (**Fig. 2**). Vertical conductivity profiles were recorded by inserting the probe into the ground, taking a reading at a particular depth, and then successively pushing the probe further into the ground up to 1.5 m depth. In addition to the *in situ* conductivity measurements, electrical properties of the ground were investigated by inverse modelling of remotely sensed resistivity measured on electrodes deployed only on the surface. Results from the *in situ* investigations are reported as electrical conductivity, whereas results obtained from the remote-sensing array are reported as electrical resistivity.

Borehole wells installed in 2001 in the Flamengo Bay (Fig. 2) were used for SGD studies (tidal effects, salinity and isotopic analyses). They consisted of perforated plastic tubes inserted into the ground. The deepest well was W0 (5 m below ground surface), the other wells were from 0.7 to 2.1 m below ground surface. Water levels were between 0.4 m and 0.8 m in wells W0, W1B, W2B and W2A, and between 1.3 and 1.5 m in wells W3B and W3A. Well W1A was without water.

Seepage chambers of three different types were used in this experiment (Bokuniewicz et al., 2008). Six manual seepage chambers were deployed for several days along a transect perpendicular from shore at Flamengo Bay (Fig. 2), starting from the low tide shoreline (with three chambers) to 44 m offshore. The respective water depths were 0 m, 0.33 m, 0.71 m, 1.07 m, 1.16 m and 1.65 m. Two other devices were placed at the low tide shoreline 19 m east and 14 m west of the transect. As manual seepage meters are very labour intensive, several types of automated seepage chambers have recently been developed (Krupa et al., 1998; Taniguchi & Iwakawa, 2001). We used a dye-dilution seepage meter, developed at Woods Hole Oceanographic Institution, which involves the injection of a coloured dye into a mixing chamber attached to a seepage meter, and measurement of its absorbance in the mixing chamber over time (Sholkovitz et al., 2003). The dye-dilution seepage meter was deployed for three days (hourly resolution for seepage) at a nearshore location (Fig. 2). Continuous-heat type automated seepage meters, as described by Taniguchi et al., 2008, were also used. SGD was continuously recorded every ten minutes at three locations (A1, A3 and A4) along the transect line shown in Fig. 2.

Multilevel piezometers with a combination of natural and artificial geochemical tracers were used for assessing groundwater seepage rates as well (Cable and Martin, 2008). Multilevel pore water samplers (multi-samplers) were installed perpendicular to the shoreline at the

Oceanography Base at distances of 2.5, 6.5, 10.5, and 35 m along the offshore transect (MS2, MS5, MS3, and MS4, respectively, **Fig. 3**). Each multi-sampler was 2.3 m long with eight sampling ports distributed between 10 and 30 cm apart along the length of the PVC pipe. After porewater sampling for isotope analysis, 100 mL of a sulphur hexafluoride (SF_6)-saturated fluorescent (green) dye solution were gently pumped through the sampling tubing connected to ports near the base of the multi-samplers. Labelled porewaters were then sampled 0.9 to 2.8 days after artificial tracer delivery at the other ports and analysed in the laboratory in order to estimate vertical advective velocities.

Salinity was continuously measured *in situ* using a 2'Micro-CTD (Falmouth Scientific Inc., USA) with a precision of ± 0.001. Temporal variations of salinity in monitoring borehole wells were measured continuously by a small "fish" DST-CTD sensor (Star-Oddi, Iceland) with precision of ± 0.01. Conductivity/salinity and temperature measurements in the field and in the laboratory were performed using portable meters. A seawater standard (Oceanor Scientific Instruments Atlantic Sea Water 35) was used for inter-instrument salinity calibrations.

In situ analysis of ^{222}Rn in seawater was carried out using a continuous alpha-spectrometry method developed by Burnett et al. (2001b), and more recently by Dulaiová et al. (2004), using an automated multi-detector system. Another system used during the mission was an *in situ* gamma-spectrometer analysing ^{222}Rn, via its daughters ^{214}Pb and ^{214}Bi, which are gamma-emitters (Povinec et al., 2001; Osvath & Povinec, 2001). The system is fully automatic and can operate without any surveillance. Spatial mapping of ^{222}Rn was carried out in several bays along the Ubatuba coast. Time series ^{222}Rn measurements were carried out in the Flamengo Bay by alpha and gamma-spectrometers at 300 m and 15 m, far from the low-tide shoreline, respectively.

3.2. Water sampling

For studying groundwater/seawater mixing in the Flamengo Bay, water samples were collected from six monitoring wells (well W1A was without water) drilled on the beach at the Oceanography Base (Fig. 2). Water samples for isotopic analysis were also collected from seepage chambers located at the low tide shoreline (SD1E), at 5 m from the shoreline (SD2), and at 32 m from the shoreline (SD5; Fig. 2). The seepage chambers were deployed long enough to be well flushed by groundwater and/or recirculated seawater. The samples from borehole wells and seepage chambers were collected during both low and high tides.

Further, water samples for isotopic analysis were collected from piezometer multi-sampler tubes located between borehole wells and seepage chambers (Fig. 2 and 3). Porewater was

collected from different horizons, between 10 and 230 cm below the sediment surface. Water samples for isotope and elemental analysis were collected in 1 L polyethylene bottles using submersible pumps (for seawater) or peristaltic pumps (for groundwater).

Groundwater samples were collected from an inland commercial well (depth 5 m) and from springs situated at the coast facing the Fortaleza, Flamengo and Picinguaba Bays, and at the Vitoria Island. River water samples were collected at the Fazenda beach in Picinguaba Bay, situated northeast of Ubatuba Bay (Fig. 1).

Seawater samples were collected in three transects (named FB, PB and V) in a series of small embayments of Ubatuba (**Fig. 4**) using R/V Albacora. Surface seawater samples were collected at ~2 m below sea surface, while bottom samples were collected 1 m above the ocean floor.

3.3. Laboratory analyses

Stable isotopes were analysed in rain, river, groundwater and seawater samples. The $\delta^{18}O$ analyses were performed using the CO_2-H_2O equilibration procedure reported in Epstein & Mayeda (1953). The δD analyses were done using H_2O-Zn reduction (Coleman *et al.,* 1982). The isotopic results were reported against the international standard VSMOW (Vienna Standard Mean Ocean Water) as defined by Gonfiantini (1978) using conventional δ notation in ‰. The precision of measurements (1σ) was ± 0.1‰ for $\delta^{18}O$ and ± 1‰ for δD. Stable isotopes of hydrogen and oxygen were analysed in the IAEA's Isotope Hydrology Laboratory in Vienna, and in the Institute of Geological and Nuclear Sciences, Lower Hutt, New Zealand.

Tritium in water samples was analysed mass spectrometrically using the ^{3}He in-growth method at the University of Miami, and by the electrolytical enrichment and liquid scintillation spectrometry in the IAEA's Isotope Hydrology Laboratory and in the Institute of Geological and Nuclear Sciences. The results are expressed in Tritium Units (1 TU represents a ratio of 1 tritium (^{3}H) atom to 10^{18} protium (^{1}H) atoms; it is equal to 118 mBq L^{-1} of water). Analyses of IAEA reference materials and regular participation in intercomparison exercises helped to assure the quality and consistency of analytical methods.

^{222}Rn in porewater samples was analyzed by liquid scintillation counting in a Packard Tri-Carb 3100TR spectrometer.

Radium isotopes were analysed by the method developed by Moore (1996) and Moore & Arnold (1996). Acrylic fibre, treated with a hot solution of saturated $KMnO_4$ was used for pre-concentration of Ra isotopes from large volume (196 L) seawater samples. After exposure to

seawater, each Mn fibre sample was dried with a stream of air and placed in a circulation system to sweep ^{219}Rn and ^{220}Rn generated by ^{223}Ra and ^{224}Ra decays in a 1.1 L scintillation cell. For the radiochemical separation of ^{226}Ra and ^{228}Ra from the sample, a carrier of stable barium (20 mg) was added. The radium was co-precipitated as Ba(Ra)SO$_4$ and transferred to a polypropylene tube and analysed by gamma-spectrometry using a HPGe germanium detector after aging for three weeks to permit ^{222}Rn and its daughters to equilibrate.

4. Results and discussion

4.1. Characterisation of SGD

4.1.1. Hydrogeology

The hydrogeology in the immediate vicinity of the Oceanography Base was studied using geologic descriptions made during the installation of the seven wells at the site, through excavations along the beach, via cores sampled in the area of the two transects, and during installation of pore water samplers offshore (Fig. 2). Onshore, the geologic materials consisted of about 3 m of colluvial material overlying highly weathered, granitic bedrock (to the total depth of the boring for well W0 at 5 m). Along the beach, 1 m of sand was found to overlie granitic boulders that made well installation difficult. In the nearshore submerged region, deposits consisted of about 0.5 m of coarse sand overlying about 0.3 m of hard sand with gravel, organics, and fines sitting atop highly weathered bedrock. At about 24 m offshore, there was a fairly abrupt transition to fine marine sediment over 2 m thick. Sediment cores revealed a thin layer (0.5 - 2 m) of sediment on top of deeply weathered crystalline bedrock. Most of the sediments, excluding the nearshore surface samples, were very poorly sorted. From the two recovered cores, most intervals contained a small amount of sand, silt, clay, and shell hash. In the offshore core, the silts and clays consisted of low permeability, making this location a poor conduit for SGD. In the nearshore core, the surficial sediments were extremely coarse grained and had been well sorted, presumably by wave action. A hydrogeologic cross-section is shown in **Fig. 5**.

Relative changes in water levels for Flamengo Bay and well W0 are presented in **Fig. 6**. The average (n = 8, for data of acceptable quality) tidal lag (a delay in tidal signal arrival at well) was 14.2 ± 1.5 hours, and the average (n = 6) tidal efficiency (a ration of tidal range in the well to that of the surface water) was 0.09 ± 0.03. Assuming an aquifer thickness of 3 m (the saturated weathered bedrock and colluvium) and a specific yield for the aquifer of 0.20, a hydraulic conductivity of 5.3 m d^{-1} was calculated from the tidal lag, which was used for estimation of SGD flux using the Darcy´s Law (see section 4.4).

Measurement of salinity is the simplest way to recognise fresh SGD in coastal waters, although it may not give full information, as SGD may be represented by a mixture of groundwater and recirculated seawater. Salinity measurements in monitoring wells and seepage chambers showed temporal variations, depending slightly on the tide level. The observed salinity levels in monitoring wells ranged from typical freshwater values (0.0 for W0) up to 34.0 for W2A, which was influenced by seawater. Salinity of water in seepage chambers varied between 20 and 31, with the lowest value measured in the seepage chamber SD1E, located on the shoreline. Even though the measured flow rates were adequate to flush the head space of other devices (such as SD1, SD5, and SD6), the measured salinities in the collected discharge remained indistinguishable from that of the ambient, open water. Saltwater must be mixed and recirculated with any freshwater SGD.

Similar salinities (between 26 and 31) were measured inside the dye-dilution chamber located on the shoreline (Fig. 2). Given an ambient bay water salinity of ~31, the lower salinities suggest that a portion of the SGD included freshwater. The rate at which this bay water is replaced is a function of the seepage rate and the headspace volume inside the seepage chamber. If we assume a headspace volume of ~5 L, a flow rate of ~16 cm d^{-1} would be required to explain the gradual freshening inside the seepage chamber, which agrees with the average flow rate (15 cm d^{-1}) of the dye-dilution method.

Freshwater salinities were found in multi-samplers MS2 and MS5 at sediment depths below 50 cm, while in MS3, below 1.5 m. MS4 did not show a contribution of fresh groundwater (**Fig. 7**). The multi-samplers data shows a presence of a thin freshwater lens in near-shore sediments, about 11 m from the low tide line. This tongue of freshwater moved within 0.4 m of the sediment-water interface, at about 8 m offshore (low tide baseline). The freshwater lens was thin and apparently confined by a hard layer, to about 1.5 m below the sediments as it moved farther offshore.

Salinity profiles measured in the Flamengo and Picinguaba Bays showed that during November 2003 (summer), the water column was well mixed. Continuous monitoring of salinity in the Flamengo Bay during November 22-26 showed variations between 33.9 and 35.3, depending on the tide level. Generally, the salinity record follows the tide record; however, sometimes delays in the salinity record were observed. Salinity along the Ubatuba coast varied from 32.0 to 34.8, showing lower values than in southwestern Atlantic waters (~ 35). The spatial variability in salinity observed both at Flamengo and Picinguaba Bays indicated possible SGD sources in the area.

4.1.2. Seepage rates

The highest seepage rates were measured by the manual seepage chambers located at the low tide shoreline (SD1, SD1E and SD1W, Fig. 2), but they were not uniform (Rapaglia, 2007). The device to the east (SD1E) recorded flow rates as high as 270 cm d^{-1}, and collection bags with a capacity of about 6 L had to be replaced every ten minutes, whereas at other locations flow rates were often sufficiently low and adequate collections were made every one to two hours. Of the three manual seepage chambers placed at the low tide shoreline (i.e. SD1E, SD1, and SD1W), the average seepage rate was 60 cm d^{-1}, ranging from 0 to 270 cm d^{-1}. The automated seepage chamber (A1) located at the shoreline recorded seepage rates as high as 350 cm day^{-1}, with an average rate of 260 cm day^{-1}. The dye-dilution seepage meter also located at the shoreline recorded an average rate of only 15 cm d^{-1}, but peaked values reached 110 cm d^{-1}.

The temporal variability was also large; measured seepage rates were found to change by as much as 160 cm d^{-1} over a 5-minute interval. Along the cross-shore transect, relatively high rates were recorded at SD1 and SD2, and again at SD5 and SD6 (**Fig. 8**). The average seepage rate at SD5 was calculated to be 8 cm d^{-1} peaking at 43 cm d^{-1} while A4, located nearby, recorded an average discharge of about 190 cm d^{-1}, ranging from 90 cm d^{-1} to 380 cm d^{-1}. Low discharge was found at site SD4 (an average rate of 5 cm d^{-1}) and at A3, situated nearby (an average rate of 4 cm d^{-1}).

The manual seepage chambers showed a temporally variable discharge but little relationship to the tide. This may be due to the collection periods limited to daytime hours only, a disadvantage overcome by the automated devices. SGD records at devices A3 and A4 did show semi-diurnal variations correlated to the tidal elevation, with higher discharges tending to occur at periods of low tide; however, the picture is very complex (**Fig. 9**). A strong and punctuated tidal modulation was seen at the dye-injection device**.** The discharge rate spiked sharply and strongly in a few hours (around the lowest tides), reaching values of 110 cm d^{-1}, against an average rate of 15 cm d^{-1} (**Fig. 10**).

The multi-sampler MS2, which was located 2.5 m from the shoreline, gave advective rates based on ^{222}Rn and SF$_6$ of about 5 cm d^{-1} and 29 cm d^{-1}, respectively. The ^{222}Rn and SF$_6$ tracers yielded at the station MS5 seepage rates of 12 and 185 cm d^{-1}, respectively, not too far from seepage rates (mean over the three-day experiment were found to be between 12 and 75 cm d^{-1}) obtained by a SD2 seepage meter installed about 1 m from MS5. Further from the shore near MS3, seepage meter SD3 yielded much lower seepage rates of about 2.9 cm d^{-1}. While the

absolute values of seepage are greater when using seepage meters than values estimated from the porewater ^{222}Rn, they are of a similar order of magnitude. The seepage meters compare especially well with estimates based on the SF$_6$ tracer experiment within 10 m wide of the nearshore area.

4.1.3. Isotopic composition

The isotopic composition of collected rain samples showed typical values expected for the Southern Hemisphere. The hydrogen isotope composition (δD) and the oxygen compositions (δ^{18}O) varied between -20.0 and -17.5‰, and between -3.7 and -3.5‰, respectively. Tritium levels measured in rainwater were around 2.5 TU. Groundwater springs and wells had δD in the range of -18.3 to -11.2 ‰, while the δ^{18}O values were between -3.9 and -3.17 ‰. Isotope results from monitoring borehole wells varied between groundwater and seawater samples, from -14.7 to 3.9 ‰ for δD, and from -3.20 to 0.49 ‰ for δ^{18}O. Wells W0 and W1B represented freshwater, while other wells showed either a mixture of fresh/seawater or seawater only (W2A, W3A, W2B and W3B). The δD values in pore water sampled from piezometer multisampler MS5 varied from -13.1 to 0.06 ‰, and δ^{18}O from -0.32 to -0.15 ‰, while MS4 showed δD values between 0.05 and 3.1 ‰, and δ^{18}O between 0.14 and 0.35 ‰. While the site MS5 was influenced by groundwater (tritium levels from 1.9 to 2.2 TU and chlorine content 0.15 - 2.5 mg g^{-1}, except for the surface which showed a presence of seawater), the site MS4 situated 35 m offshore showed tritium (1.0 – 1.4 TU) and chlorine (~19 mg g^{-1}) levels typical for seawater.

The water samples collected in the seepage chambers showed isotopic composition between seawater and groundwater. The δD results were between 0.4 and 0.6 ‰, and δ^{18}O between -0.07 and 0.0 ‰, documenting that recirculated seawater with a small admixture of groundwater has been playing a dominant role in the seepage. The tritium concentration (2.1 TU) measured in the seepage chamber SD1E was similar to the one measured in multi-sampler MS5, situated only 6.5 m from the shoreline where SD1E was located. A time series of water samples collected in the seepage chamber SD1E showed Cl content of ~15 mg g^{-1}, confirming a presence of freshwater concentration of which did not change with tide. Seepage chambers SD2 and SD5 were even more influenced by seawater (as expected from samples collected in multi-samplers), having δD values between 0.0 and 1.7 ‰, and δ^{18}O between -0.12 and 0.15 ‰.

The isotope composition of river water sampled at Fazenda Beach (Picinguaba Bay) varied from -15.6 to -9.3 ‰ for δD, and between -3.61 and -2.92 ‰ for δ^{18}O, showing values which were close to the rain values. Tritium levels in the river water were around 2.5 TU, influenced by

the isotopic composition of the rainwater. Tritium levels in groundwater samples ranged from 2.1 to 2.7 TU. The groundwater spring found at the Oceanographic Base showed similar stable isotope and tritium levels to the groundwater spring found on the road about 10 km from the Base (used by local population as a source of drinking mineral water), and is one of the groundwater end-member candidates.

Stable isotopes in seawater samples were characterised by significant variability and enrichment in ^{18}O, which were very different from groundwater samples. Seawater samples were mostly from 1.0 to 4.6 ‰ for δD, and from -0.02 to 0.53 ‰ for δ^{18}O. Tritium levels in visited bays varied between 0.9 and 2.7 TU. They did not show any correlation with sampled water depth, which varied between 2 and 40 m.

The Local Meteoric Water Line (LMWL) for the São Paulo region was constructed on the basis of the IAEA's GNIP (Global Network of Isotopes in Precipitation) database (www.IAEA.org). The calculated LMWL can be represented by the equation δD = 8.1 δ^{18}O + 5.2, which can be compared with the Global Meteoric Water Line (GMWL) defined after Craig (1961) as δD = 8 δ^{18}O + 10. In the δD versus δ^{18}O diagram groundwater springs, rain, river and some of the monitoring wells data are grouped above the GMWL, while the seawater data are below this line (**Fig. 11**). The LMWL calculated for the São Paulo inland region does not fit well with the data set, probably due to an influence of the sea on the isotopic composition of rains. The regression line through the groundwater-seawater data (correlation coefficient r^2 = 0.97, P < 0.0001) shows a lower slope than that of the GMWL and LMWL. This could be due to seawater-atmospheric water vapor interactions and non-equilibrium isotopic fractionation of groundwater after its infiltration and underground circulation. Groundwater is depleted in ^{18}O with respect to the VSMOW, while the seawater samples are highly enriched in ^{18}O. The diagram in Fig. 11 confirms that groundwater samples are well separated from seawater samples. Therefore, in the majority of cases, there has not been a significant mixing of groundwater with seawater at the visited sites. The water samples from monitoring wells and seepage chambers are situated between the main groups of samples, representing mixtures of groundwater and seawater. The variability in D and ^{18}O enrichment may be caused by different seawater contributions to the collected samples as recirculated seawater is playing dominant role in coastal groundwater/seawater interactions. Therefore the original composition of the groundwater component entering the sea floor may be different.

The isotope composition (δD, δ^{18}O and ^{3}H) of submarine waters is characterised by a significant variability and heavy isotope enrichment, with δD values between -15 and 4.5 ‰,

$\delta^{18}O$ between -3.20 and 0.5 ‰, and ^3H between 1.0 and 2.2 TU. The groundwater end-member can be represented by groundwater springs found at the Oceanography Base, which showed similar isotopic compositions (δD values between -18 and -12 ‰, $\delta^{18}O$ between -3.9 and -3.2 ‰, and ^3H between 2.0 and 2.7 TU). On the other hand, the seawater end-member may be represented by open sea samples collected between the coast and the Vitoria Island, with δD and $\delta^{18}O$ values around 3.0 and 0.5 ‰, respectively, and ^3H around 1.2 TU. By using a simple mixing model with these two end-members, we can calculate that the contribution of fresh groundwater in submarine waters may vary from a small percentage to 17 % only, depending on the location and the tide level. Hence, the submarine waters may be represented by coastal groundwater and recirculated seawater with small proportions of groundwater in the mixture.

4.2. Spatial distribution of SGD

Geoelectric measurements allow for predictions of entry points of fresh SGD. While it is not possible to derive absolute SGD fluxes from such measurements, the relative distribution of SGD can be investigated in detail, especially where seepage or discharge follows preferential flow paths, which can guide the positioning of seepage chambers and piezometers. A high-resolution transect measured at Flamengo Bay, interpolated from 130 single-point measurements recorded on electrodes inserted into the ground at different locations along the transect, is presented in **Fig. 12.** The presented transects document a highly dynamic groundwater-seawater system in Flamengo Bay during three days of measurements. The significantly reduced ground conductivity close to the sediment surface at around 23-25 m distance suggests a greater influence of fresh SGD at this location than along other parts of the transect. A manual seepage meter, which was deployed at this location subsequent to the conductivity investigations, confirmed both the highest flow rate and lowest salinity discharge along the transect. Without the conductivity investigations, only the seepage meters at a 20-m and 31-m distance would have been deployed, and thus the total flow rate would have been significantly underestimated.

Simultaneously recorded conductivity and resistivity transects at Fazenda beach (Picinguaba Bay) reveal similar features of the subsurface distribution of seawater and freshwater (Fig. 12b). Despite the very different spatial scales of the operation of the methods (centimeter vs. meter scale), both methods detected the general features of three low conductivity/high resistivity regions along the beach-parallel profile. The transect was recorded across a dry creek on the beach. It is likely that the low conductivity/high resistivity central region of the transect represents the alluvial aquifer of the creek.

A distribution of ^{222}Rn in surface seawater measured by alpha and gamma-spectrometers was used for estimation of spatial distribution of SGD in the Flamengo and Picinguaba Bays. In the Flamengo Bay, the ^{222}Rn activity concentrations varied between 2 and 200 Bq m^{-3}, and the highest values were found close to the Oceanography Base and at Perequê-Mirim beach. Four stations visited in Picinguaba Bay showed ^{222}Rn activity concentrations between 50 and 140 Bq m^{-3}. An inverse relationship between the observed ^{222}Rn activity concentration of surface seawater and salinity is demonstrated in **Fig. 13** for Flamengo and Picinguaba Bays (r^2 = 0.93, P = 0.035 and r^2 = 0.92, P = 0.039, respectively). The negative correlation indicates that waters with lower salinity have higher ^{222}Rn concentrations, due to an admixture of groundwater. The ^{222}Rn activity concentrations at Flamengo Bay were up to three times higher than in Picinguaba Bay (at similar salinities), which suggests different sources of groundwater in the bays.

Generally, there was a rapid loss of ^{222}Rn from groundwater to saline waters, as its levels in the monitoring borehole wells in Flamengo Bay were much higher (from 4 to 25 kBq m^{-3} for W1B and W0, respectively). Elevated ^{222}Rn activity concentrations were also observed in multi-samplers (e.g. for MS5 from 4 to 16 kBq m^{-3}, depending on the pore water sampling depth). The ^{222}Rn versus salinity plot (**Fig. 14**) illustrates the rapid loss of Rn from brackish or saline pore waters.

Variations in concentrations of Ra isotopes in surface seawater were used for evaluation of possible trends in SGD distribution with offshore distance. The ^{223}Ra activity concentrations varied from 0.04 to 0.2 Bq m^{-3}, ^{224}Ra from 0.2 to 3.5 Bq m^{-3}, ^{226}Ra from 0.8 to 1.7 Bq m^{-3} and ^{228}Ra from 1.5 to 3 Bq m^{-3}. Much higher Ra concentrations were observed in the monitoring borehole well W2A: 1.4 Bq m^{-3}, 73 Bq m^{-3}, 1.6 Bq m^{-3} and 8.9 Bq m^{-3} for ^{223}Ra, ^{224}Ra, ^{226}Ra and ^{228}Ra, respectively, documenting that this well was influenced by groundwater. The highest Ra activities in seawater were measured in the nearshore waters of Flamengo Bay, where high ^{222}Rn concentrations were also found. However, the Vitoria transect samples (Fig. 4) show that there is no consistent trend of decreasing activity with offshore distance. ln Ra activity as a function of offshore distance does not show a decreasing trend for samples collected beyond 5 km (**Fig. 15**).

These transects were used for estimation of residence time of waters within 25 km offshore as described in detail by Moore & Oliveira (2008). The calculated age vs. distance offshore for collected samples is shown in **Fig. 16.** Samples collected in the bays have ages in the range 2 to 10 days, relative to the water collected in the seepage chamber. Further offshore, there is a trend of increasing age with distance, and between 10 and 25 km the ages are in the range 7 to 15 days. The fact that the ages do not follow a single trend with offshore distance must be due to the ruggedness of the coastline, where many small bays and small islands interrupt simple mixing

patterns. As water circulates through these bays, small scale eddies may develop and propagate onto the shelf. Changes in wind direction must also have a strong effect on the eddy formation and the circulation.

4.3. Temporal variations of SGD

Continuous radon measurements of coastal waters (2 m water depth) were made using alpha-spectrometry at a fixed location from a float located about 300 m from the Oceanography Base, from November 15 to 20 (**Fig. 10**). Generally, an inverse relationship between the ^{222}Rn activity concentration and tide in Flamengo Bay was found. The observed temporal changes in ^{222}Rn concentration were from 20 to 100 Bq m^{-3}. A direct comparison of continuous ^{222}Rn measurements and advection rates measured by the dye-dilution seepage meter shows some interesting patterns. While the two instruments only overlapped about 2.5 days during the weeklong experiment, there are clear indications that both measurements are responding to either tidally induced or modulated forcing. The main peaks in both data sets have a 24-hour period and correspond to the lowest low tide each day. There are also indications in both records of secondary peaks occurring at the higher low tide. This is more obvious in the seepage meter record, but the radon does show a clear shoulder during the evening low tide on November 19th. It is encouraging that these two independent tools respond in such a similar manner to the same process. The seepage meter measured flow directly from a small portion of seabed close to shore, while the radon was measured in the overlying water a few hundred meters away and presumably with a much larger sphere of influence.

A time series of ^{222}Rn activity concentration in seawater, salinity, and tide were also recorded from November 22nd to 26th in Flamengo Bay using the *in situ* gamma-spectrometer, situated 15 m offshore the Oceanography Base, where the largest SGD fluxes were observed by the seepage meters group. The ^{222}Rn activity concentrations varied between 1 and 5.1 kBq m^{-3}, while the tide level varied between 4.4 and 5.6 m. The ^{222}Rn time series in Flamengo Bay showed a weak negative correlation of its activity concentration with tidal stage, when during decreasing sea level ^{222}Rn concentration was slightly increasing, and opposite, during high tides ^{222}Rn concentration was decreasing. An observation of a few hours occured between the tide minimum and ^{222}Rn activity concentration maximum (and opposite). However, this usual inverse relationship between the ^{222}Rn activity concentration in seawater and tide/salinity was not observed during November 22nd, despite large variations in water levels and high salinities. The observed salinities (from 34.7 to 35.3) were much higher than during November 25th and 26th

(showing, however, small changes with tide during this time), which would indicate that the Bay on November 22nd was predominantly occupied by waters from the open sea (SACW), having higher salinity (35-36) and lower ^{222}Rn concentration. The expected inverse relationship between the ^{222}Rn activity concentration in seawater and tide/salinity was seen from November 23rd to 25th, when the Bay was again under the influence of groundwater discharge.

A fifty times higher ^{222}Rn concentrations observed by gamma-spectrometry than by alpha-spectrometry may be due to the position of the gamma-spectrometry monitoring site, which was closer to the shoreline (15 m vs. 300 m). Around this site, large SGD fluxes were observed by seepage meter groups. The piezometer group also reported high ^{222}Rn concentrations in pore water (up to 15 kBq m^{-3} at the site MS5). The ^{222}Rn concentrations measured with an underwater gamma-ray spectrometer at other sites in the Flamengo Bay were comparable with the results obtained by alpha-spectrometry.

4.4. Estimation of SGD fluxes

There were wide spatial and temporal variations of SGD fluxes as measured by seepage chambers. The manual seepage chambers recorded SGD fluxes between 0 and 270 cm d^{-1}, while the SGD rates registered by the automated seepage chambers were between 2 and 110 cm d^{-1} for the dye-dilution seepage meter, and between 4 and 360 cm d^{-1} for the automated seepage chambers. The SGD fluxes found at site MS3 by the piezometer group were 9-24 cm d^{-1} (estimated from pore water inventories), and 50 cm d^{-1} (estimated using artificial tracers).

Several approximations have to be made for estimation of SGD fluxes from measured ^{222}Rn concentrations (Burnett and Dulaiova, 2003; Burnett et al., 2008; Povinec et al., 2008). SGD rates estimated from the continuous alpha-spectrometry measurements of ^{222}Rn decay products had a similar pattern (Fig. 17), as seen by some of the manual and automated seepage meters deployed at the same time. Over a 109-hour period, the estimated SGD flux ranged from 1 to 29 cm d^{-1}, with an average of 13±6 cm d^{-1}. The average seepage rate is very close to the average calculated from the dye-dilution seepage meter of 15 cm d^{-1}, although that device indicated a much broader range – from about 2 up to 110 cm d^{-1} - for short periods during the lowest tides. Most of the seepage spikes that were observed by alpha-spectrometer occurred during the lowest tides, with the exception of the peak around noon on November 17th. Inspection of the rainfall record (Fig. 17b) shows that this was also a period when there was a significant amount of rain which washed out radon decay products from the air. Thus, this extra peak may be due to a rapid response of a shallow aquifer to the rainfall event.

The SGD fluxes estimated from underwater gamma-spectrometry (Fig. 18) varied during November 22-26, between 8 and 35 cm d^{-1}, with an average value of 21±10 cm d^{-1}. The obtained SGD flux is similar to that obtained between November 16th and 20th, using the alpha-spectrometry method (the average value 13±6 cm d^{-1}). As we already mentioned, much larger SGD fluxes (over 300 cm d^{-1}) were measured at the low tide shoreline by manual and continuous seepage meters groups; however, comparable results with radon data were obtained for a site situated about 10 m from the shoreline. Generally, these results showed large temporal and spatial variations in SGD fluxes observed in the small bay area. At the monitoring site the contribution of freshwater in seawater varied between a small percentage to 20%, with an average value of 10%. However, with offshore distance, as documented by isotopic composition and clear separation of groundwater and seawater in collected samples (and due to the absence of samples collected in bays with higher groundwater contribution), there was only a small contribution of freshwater in the submarine groundwater discharge.

Another possibility to calculate the discharge of freshwater per unit width of shoreline is using the Darcy's Law

$$Q/w = -K \, b \, dh/dl,$$

where Q is discharge, w is the width of shoreline, K is the hydraulic conductivity, b is the aquifer thickness, and dh/dl is the hydraulic gradient. The hydraulic gradient on land was measured between freshwater wells W0 and W1B. With a water level change of 0.13 m over a distance of 12.3 m, the hydraulic gradient was calculated to be 0.011, representing a single snapshot of the gradient at that particular moment. This gradient will change at different times in the tidal cycle as the tidal signal is propagated inland. The hydraulic gradient could vary with time by a factor of two from the value given. The aquifer thickness was taken as approximately 3 m, and a range of hydraulic conductivity values was determined (see section 4.1). The most reasonable estimate of the SGD flux, based on the hydraulic conductivity values determined from the tidal signal propagation, ranged over an order of magnitude from 0.17 to 1.6 m^3 d^{-1} per meter of shoreline. While the fresh SGD is probably not evenly distributed across the 24 m of coarse sediment nearest shore, an estimate of the average seepage rate can be made by dividing the SGD by the 24 m distance. The net, upward, freshwater seepage rate thus estimated is 0.7 to 70 cm d^{-1}. As freshwater comprises in average only 10% of the SGD (as obtained from isotope tracers), the total SGD flux could be between 7 and 700 cm d^{-1}.

Using the average nearshore SGD flux estimated from ^{222}Rn measurements (13±6 cm d^{-1}), the total shoreline length of ~40 km and the offshore distance of SGD manifestation of ~50 m, the total nearshore SGD flux is ~3 x 10^5 m^3 d^{-1}. Using ^{228}Ra activity concentration measured in two

seepage chambers (70 Bq m^{-3}) we can estimate the nearshore SGD ^{228}Ra flux of about 2 x 10^7 Bq d^{-1}. For the study area (V = 3.5 x 10^9 m^3) and the estimated residence time of ten days, the nearshore SGD flux can support an excess ^{228}Ra inventory of about 2 x 10^8 Bq, which is only 10% of the measured ^{228}Ra enrichment. This would imply that the manifestation of SGD with offshore distance based on the local estimates in Flamengo Bay has been underestimated (as also indicated by nutrient data, Povinec et al., 2008), as well as some significant sites of nearshore SGD, which has not been included in the assessment. There are clear indications that SGD may occur as far as 23 km offshore at Vitoria Island.

The SGD fluxes estimated by various methods are listed in **Table 1**, which represents a valuable intercomparison of very different methods that yielded comparable results. The observed irregular distribution of SGD seen at Ubatuba is a characteristic of fractured rock aquifers. The bay floor sediments were sandy and not noticeably different from place to place in the study area. However, bedrock is exposed at the shoreline and an irregular rock surface was encountered at shallow depths offshore. For example, investigators could drive probes to a depth of a few meters in some places but less than half a meter at adjacent locations. The water feeding the SGD is supplied to the bottom of the thin blanket of unconsolidated sediment through a fractured system and concentrated (or dispersed) along the irregular surface of the buried rock. Presumably, this is fresh groundwater working its way seaward through the fractured rock.

4.5. Comparison with previous SGD investigations

When comparing the obtained results with similar measurements recently carried out offshore southeastern Sicily (Povinec et al., 2006a), we observe several differences:

i) At the Sicilian site, the ^{222}Rn concentrations strongly depended on the tide, although only small changes in the tide were observed (10 cm in Sicily vs. 120 cm in Brazil). The ^{222}Rn concentrations in seawater at the Sicilian and Brazilian sites were very similar, between 2 and 5 kBq m^{-3}, and 1 and 5 kBq m^{-3}, respectively. In contrast to the Sicilian sites, which represent a typical karstic region with low concentrations of U and Th, the Brazilian sites are coastal areas characterised by crystalline rocks, where the concentrations of ^{238}U and ^{232}Th in collected rock and sediment samples were higher, at least by a factor of 5. Therefore, higher ^{222}Rn activity concentrations in groundwater and seawater along the Ubatuba coast would be expected.

ii) The observed [222]Rn levels and stable isotope data in the Flamengo and Picinguaba Bays indicate that the admixture of freshwater in submarine waters is much lower than in Sicily, where levels up to 50% were observed. SGD in the Ubatuba region is mostly represented by recirculated seawater, having a lower [222]Rn concentration. At the monitoring site, the contribution of freshwater in seawater varied between a small percentage to 20%, with an average value of 10%. However, with offshore distance, as documented by isotopic composition and clear separation of groundwater and seawater in collected samples, there was even smaller contribution of freshwater in the submarine groundwater discharge.

iii) Integrated coastal SGD flux estimated for the Sicilian coast is about 5×10^6 m^3 d^{-1} per km of the coast, which is more than two orders of magnitude higher than for the Ubatuba coast.

iv) It appears from the presented observations that the advection of pore water fluids across the seabed in the Flamengo Bay is not a steady state but episodic with a period that suggests tidal forcing or modulation. This is very similar to observations reported from other environments (e.g., Burnett et al., 2002; Sholkovitz et al., 2003; Burnett et al., 2006).

5. Conclusions

The main observations made in this study could be summarised as follows:

i) Large fluctuations of SGD fluxes were observed at sites situated only a few meters apart (from 0 cm d^{-1} to 360 cm d^{-1}), as well as during a few hours (from 2 cm d^{-1} to 110 cm d^{-1}), strongly depending on the tidal fluctuations detected by a multitude of methods. A reasonable agreement has been obtained in the estimation of SGD fluxes, which were obtained by manual and automate seepage meters, piezometers, radon measurements and hydrogeologic modelling. The average nearshore SGD rate estimated from the continuous alpha and gamma-spectrometry measurements of [222]Rn decay products was 17 ± 10 cm d^{-1}. The irregular distribution of SGD seen at Ubatuba is a characteristic of fractured rock aquifers.

ii) The geoelectric probing helped to understand the spatial distribution of different water masses present within the substrate, and prove to be a useful tool for guiding seepage measurements.

iii) The isotopic composition of submarine waters (δD, δ^{18}O, ^{3}H) was characterised by significant variability and heavy isotope enrichment indicating that the contribution of groundwater in submarine waters varied from a small percentage to 20%, depending on the location and tide level. With increasing offshore distance, this contribution became negligible.

iv) A spatial distribution of ^{222}Rn activity concentration offshore Ubatuba has revealed changes between 2 and 200 Bq m^{-3}, which anticorrelated with observed salinities. A time series of ^{222}Rn activity concentration in the Flamengo Bay (1 to 5 kBq m^{-3}) confirmed a negative correlation between the ^{222}Rn activity concentration and tide/salinity. The variations in ^{222}Rn activity concentration were caused by sea level changes as tide effects induce variations of hydraulic gradients. A lower ^{222}Rn activity concentration during high tides may also be due to a dilution of bay waters by offshore waters. At the monitoring site, the contribution of freshwater in the seawater varied between a small percentage and 20%, with an average value of 10%.

v) The radium isotopes data showed scattered distributions with offshore distance, which imply that coastal waters in small bays were influenced by local currents and groundwater/seawater mixing. This has also been confirmed by a relatively short residence time of 1-2 weeks for waters within 25 km of the shore, as obtained by short-lived radium isotopes. The ages do not follow a single trend with offshore distance which must be due to the ruggedness of the coastline, where many small bays and small islands interrupt simple mixing patterns. As water circulates through these bays, small scale eddies may develop and propagate onto the shelf. Changes in wind direction must also have a strong effect on the eddy formation and the circulation.

vi) Using the average SGD flux estimated from ^{222}Rn measurements, the total shoreline length of ~40 km and the offshore distance of SGD manifestation of ~50 m, the total nearshore SGD flux is about 3×10^5 m^3 d^{-1}. By using ^{228}Ra activity concentration measured in seepage chambers, we estimated the nearshore SGD ^{228}Ra flux of about 2×10^7 Bq d^{-1}. For the study area of about 3.5×10^9 m^3 and the estimated residence time of 10 days, the nearshore SGD flux can support an excess ^{228}Ra inventory of about 2×10^8 Bq, which is only 10% of the measured ^{228}Ra enrichment. This would imply that

SGD with offshore distance based on the local estimates in Flamengo Bay may have been underestimated (i.e., there is probably significant offshore SGD).

Large changes in isotopic composition of seawater observed in a relatively small area document the importance of the isotopic characterisation of coastal waters for a better understanding of groundwater/seawater interactions in the region. Discussed intercomparison exercises produced either a reasonable agreement between different techniques or displayed variations that could be explained by the geologic setting. SGD in the Ubatuba area is fed by coastal groundwater and recirculated seawater with small admixtures of groundwater, with potential environmental concerns and implications on the management of freshwater resources in the region.

Acknowledgements

References

Bokuniewicz, H. 1992. Analytical description of sub-aqueous groundwater discharge. *Estuaries,* 15, 458-464.

Bokuniewicz, H., Taniguchi, M., Ishitoibi, T., Charette, M., Allen, M., Kontar, E.A. 2008. Direct measures of submarine groundwater discharge over a fractured rock aquifer in Ubatuba, Brazil. *Estuarine, Coastal and Shelf Science*, 76, 466-472.

Burnett, W.C., Chanton, J., Christoff, J., Kontar, E., Krupa, S., Lambert, M., Moore, W., O'Rourke, D., Paulsen, R., Smith, C., Smith, L. & Taniguchi, M. 2000. Assessing methodologies for measuring groundwater discharge to the ocean. *EOS,* 83, 117-123.

Burnett, W.C., Taniguchi, M., Oberdorfer, J.A. 2001a. Assessment of submarine groundwater discharge into the coastal zone. *Journal of Sea Research* 46, 109-116.

Burnett, W.C., Kim, G. & Lane-Smith, D. 2001b. A continuous radon monitor for assessment of radon in coastal ocean waters. *Journal of Radioanalytical and Nuclear Chemistry* 249, 167-172.

Burnett, W.C. & Dulaiova, H. 2003. Estimating the dynamics of groundwater input into the coastal zone via continuous radon-222 measurements. *Journal of Environmental Radioactivity* 69, 21-35.

Burnett, W.C. & Dulaiova, H. 2006. Radon as a tracer of submarine groundwater discharge into a boat basin in Donnalucata, Sicily. *Continental Shelf Research* 26, 862-873.

Burnett, W.C., Aggarwal, P.K., Aureli, A., Bokuniewicz, H., Cable, J.E., Charette, M.A., Kontar, E., Krupa, S., Kulkarni, K.M., Loveless, A., Moore, W.S., Oberdorfer, J.A., Oliveira, J., Ozyurt, N., Povinec, P.P., Privitera, A.M.G., Rajar, R., Ramessur, R.T., Scholten, J., Stieglitz, T., Taniguchu, M., Turner, J.V. 2006. Quantifying submarine groundwater discharge in the coastal zone via multiple methods. *The Science of the Total Environment* 367, 498-543.

Burnett, W.C., Peterson, R. Moore, W.S., Oliveira, J. 2008. Radon and radium isotopes as tracers of submarine groundwater discharge – results from the Ubatuba, Brazil SGD assessment intercomparison. *Estuarine, Coastal and Shelf Science*, 76, 501-511.

Cable, J., Burnett, W., Chanton, J., Weatherly, G. 1996. Estimating groundwater discharge into the northeastern Gulf of Mexico using ^{222}Rn, *Earth and Planetary Science Letters*, 144: 591-604.

Cable, J., Martin, J., Swarzenski, P., Lindenberg, M., Steward, J., 2004, Advection within shallow pore waters of a coastal lagoon, *Ground Water* 42: 1011-1020, doi: 10.1111/j.1745-6584.2004.tb02640.

Cable, J.E. & Martin, J.B. 2008. In situ evaluation of nearshore marine and fresh porewater transport into Flamengo Bay, Brazil. *Estuarine, Coastal and Shelf Science*, 473-483.

Coleman, M.L., Sheppard, T.J., Durham, J.J., Rouse, J.E., Moore, G.R. 1982. Reduction of water with zinc for hydrogen isotope analysis. *Anal. Chem.* 54, 993-995.

Craig, H. 1961. Isotopic variation in meteoric waters. *Science* 133, 1702-1703.

Dulaiova, H., R. Peterson, and W.C. Burnett, 2005. A multi-detector continuous monitor for assessment of ^{222}Rn in the coastal ocean. J. Radioanal. Nucl. Chem. 263, 361-365.

Epstein, S. & Mayeda, T., 1953. Variation of O^{18} content of waters from natural sources. *Geochimica et Cosmochimica Acta* 4, 213-224.

Gonfiantini, R., 1978. Standards for stable isotope measurements in natural compounds. *Nature* 271, 534-536.

Kim, G. & Hwang, D.W., 2002. Tidal pumping of groundwater into the coastal ocean revealed from submarine Rn-222 and CH_4 monitoring. Geophys. Res. Lett. 29, 10.1029/2002 GL015093.

Krupa, S.L., T.V. Belanger, H.H. Heck, J.T. Brok and B.J. Jones, 1998. Krupa seep – the next generation seepage meter, J. Coastal Res. 25, 210-213.

Mahiques, M.M. 1995. Sedimentary dynamics of the bays off Ubatuba, State of São Paulo. *Boletim do Instituto Oceanographico, São Paulo* 43(2), 111-122.

Martin, J., Cable, J., Swarzenski, P., Lindenberg, M. 2004. Enhanced submarine ground water discharge from mixing of porewater and estuarine water. *Ground Water* 42, 1001-1010.

Martin, J., Cable, J., Smith, C., Roy, M., Cherrier, J. 2007. Magnitudes of submarine groundwater discharge from marine and terrestrial sources: Indian River Lagoon, Florida, *Water Resources Research*, 43, W05440, doi:10.1029/2006WR005266.

Mesquita, A.R. 1997. Marés, circulação e nível do mar na Costa Sudeste do Brasil. Relatório Fundespa, São Paulo.

Moore, W.S. 1996. Large groundwater inputs to coastal waters revealed by Ra-226 enrichments. *Nature* 380, 612-614.

Moore, W.S., Arnold, R. 1996. Measurement of ^{223}Ra and ^{224}Ra in coastal waters using a delayed coincidence counter. *Journal of Geophysical Research* 101, 1321-1329.

Moore, W.S. 2000. Ages of continental shelf waters determined from ^{223}Ra and ^{224}Ra. *Journal of Geophysical Research* 105, 22117-22122.

Moore, W.S., Wilson, A.M. 2005. Advective flow through the upper continental shelf driven by storms, buoyancy and submarine discharge. *Earth and Planetary Science Letters* 235, 564-576.

Moore, W.S. 2006. Radium isotopes as tracers of submarine groundwater discharge in Sicily. *Continental Shelf Research* 26, 852-861.

Moore, W.S. & Oliveira, J. 2008. Determination of residence time and mixing processes of the Ubatuba, Brazil, inner shelf waters using natural Ra isotopes. *Estuarine, Coastal and Shelf Science*, 512-521.

Oberdorfer, J.A., Charette, M., Allen, M., Martin, J.B., Cable. J.E., 2008. Hydrogeology and geochemistry of near-shore submarine groundwater discharge at Flamengo Bay, Ubatuba, Brazil. *Estuarine, Coastal and Shelf Science*, 457-465.

Oliveira, J., Burnett, W.C., Mazzilli, B.P., Braga, E.S., Farias, L.A., Christoff, J. & Furtado, V.V. 2003. Reconnaissance of submarine groundwater discharge at Ubatuba coast, Brazil, using ^{222}Rn as a natural tracer. *Journal of Environmental Radioactivity 69,* 37-52.

Oliveira, J., Charette, M., Allen, M., Braga, E. S., Furtado, V.V. 2006a. Coastal water exchange rate studies at the southeastern Brazilian margin using Ra isotopes as tracers. In: *Radionuclides in the Environment*, (Povinec, P.P., Sanchez-Cabeza, J.A., Eds.). Elsevier, Amsterdam, Netherlands, pp. 345-359.

Oliveira, J., Elísio, A.C.R., Teixeira, W.E., Peres, A.C., Burnett, W.C., Povinec, P.P., Somayajulu, B.L.K., Braga, E.S., Furtado, V.V. 2006b. Isotope techniques for assessment of submarine groundwater discharge and coastal dynamics in Ubatuba coastal areas, Brazil. *Journal of Coastal Research* SI39, 1084-1086.

Osvath, I. & Povinec, P.P. 2001. Seabed gamma-ray spectrometry: applications at IAEA-MEL. *Journal of Environmental Radioactivity* 53, 335-349.

Povinec, P.P., La Rosa, J., Lee, S.-H., Mulsow, S., Osvath, I. Wyse, E. 2001. Recent developments in radiometric and mass spectrometry methods for marine radioactivity measurements. *Journal of Radioanalytical and Nuclear Chemistry* 248, 713-718.

Povinec, P., Aggarwal, P., Aureli A., Burnett, W. C., Kontar, E. A., Kulkarni, K. M., Moore, W. S., Rajar, R., Taniguchi, M., Comanducci, J.-F., Cusimano, G., Dulaiova, H., Gatto, L., Hauser, S., Levy-Palomo, I., Ozorovich, Y. R., Privitera, A. M. G. & Schiavo, M. A. 2006a. Characterisation of submarine ground water discharge offshore south-eastern Sicily – SGD Collaboration. *Journal of Environmental Radioactivity* 89, 81-101.

Povinec, P.P., Comanducci, J.-F., Levy-Palomo, I., & Oregioni, B. 2006b. Monitoring of submarine groundwater discharge along the Donnalucata coast in the south-eastern Sicily using underwater gamma-ray spectrometry of radon decay products. *Continental Shelf Research* 26, 874-884.

Povinec, P.P., Oliveira, J., Braga, E.S., Comanducci, J-F., Gastaud, J., Groening, M., Levy-Palomo, I., Morgenstern, U., Top, Z., 2008. Isotopic, trace element and nutrient characterization of coastal waters from Ubatuba inner shelf area, southeastern Brazil. *Estuarine, Coastal and Shelf Science*, 522-542.

Rapaglia, J.P. 2007. Using Direct Measurements of Submarine Groundwater Discharge to Investigate the Coupling Between Surface and Pore Waters. Stony Brook University, Marine Sciences Research Center, Ph.D. Dissertation: 246pp.

Sholkovitz, E.R., C. Herbold, and M.A. Charette, 2003. An automated dye-dilution based seepage meter for the time-series measurement of submarine groundwater discharge. Limnol. Oceanogr. Methods 1, 17-29.

Stieglitz, T. 2005. Submarine groundwater discharge into the near-shore zone of the Great Barrier Reef, Australia. *Marine Pollution Bulletin* 51, 51-59.

Stieglitz, T., Taniguchi, M., Neylon, S., 2008. Spatial variability of submarine groundwater discharge, Ubatuba, Brazil. *Estuarine, Coastal and Shelf Science*, 493-500.

Taniguchi, M. and H. Iwakawa, 2001. Measurements of submarine groundwater discharge rates by a continuous heat-type automated seepage meter in Osaka Bay, Japan. *J. Groundwater Hydrology* 43, 271-277.

Taniguchi, M., Burnett, W.C., Cable & J.E., Turner, J.V., 2002. Investigation of submarine groundwater discharge, *Hydrological Processes,* 16, 2115-2129.

Taniguchi M., Stieglitz, T., Ishitobi, T., 2008. Temporal variability of water quality of submarine groundwater discharge in Ubatuba, Brazil. *Estuarine, Coastal and Shelf Science*, 484-492.

Weinstein, Y., Less, G., Kafri, U. & Herut, B. 2006. Submarine groundwater discharge in the Southeastern Mediterranean. In: *Radionuclides in the Environment*, (Povinec, P.P., Sanchez-Cabeza, J.A., Eds.). Elsevier, Amsterdam, Netherlands, pp. 360-372.

Table 1

Ranges and mean values of SGD fluxes estimated during the Brazil intercomparison (November, 2003) by different approaches in the nearshore zone off the Oceanography Base in Flamengo Bay

	Seepage meters					Other	
	Manual	Continuous heat	Dye-dilution	Radon α-spec.	γ-spec.	Multi-samplers	Darcy´s Law
Range (cm d^{-1})[*]	0-270	0-360	2-110	1-29	8-35	28-180[#]	7-700
Mean (cm d^{-1})		260 (A1[x])	15±19[$]	13±6	21±10	88±84	
		3 (A3)					
		190 (A4)					

[*] The unit is cm^3/cm^2 day.
[#] SF$_6$ tracer-derived seepage rates are minimums.
[x] A1, A3 and A4 indicates locations of seepage meters.
[$] The standard deviations reported reflect variations of the measured seepage rates.

List of Figures

Figure 1. Ubatuba coast in the south-eastern Brazil with typical geomorphologic features. The SGD work was mostly carried out in Flamengo Bay (which is hosting the Oceanography Base) and in Piciguaba Bay. (a) Location map, and false-colour Landsat image of the study sites (b) Flamengo Bay and (c) Fazenda Beach. Study locations are marked. Image Source: NASA.

Figure 2. (a) Monitoring site in Flamengo Bay in front of the Oceanography Base. Positions of monitoring borehole wells (W), manual seepage chambers (SD), automated seepage chambers (A) and WHOI, piezometer multisamplers (MS) and the underwater gamma-ray spectrometer (GS) are shown together with the low tide shoreline. (b) Photo of the site showing borehole wells (e.g. W1B is seen in the rigth bottom corner), seepage chambers with buoys, and rods for geoelectric probing.

Figure 3. A schematic cross-section of the field site with multi-level piezometers (depths of tracer injection are indicated by arrows).

Figure 4. Sampling sites offshore Ubatuba. Seawater was sampled along several transects offshore Flamengo, Forteleza and Mar Virado Bays up to Vitoria Island. The position of the Oceanography Base (B) in Flamengo Bay is also shown.

Figure 5. Conceptual model of geology and hydrogeology at transect B at the Oceanography Base in Flamengo Bay.

Figure 6. Tidal signal in Flamengo Bay and the freshwater borehole well W0.

Figure 7. Pore water salinity versus depth in multi-level piezometer transect extending offshore (Fig. 3). Low saline fluid underlies salt water in upper section of sediment. Tongue of freshwater extends offshore to approximately 10.5 m from the low tide line near MS3. Freshwater signal has disappeared from pore waters by about 26 m offshore.

Figure 8. SGD measured along the transect offshore (consult Fig. 2 for positions of seepage chambers). Seepage chambers SD1W and SD1E, situated west and east of the SD1 on the

shoreline, showed fluxes up to 2 and 4 times higher than SD1, respectively. Time is in hours starting at midnight on 17 November 2003. Note the difference in the scale of the vertical axes.

Figure 9. Temporal changes in tide, SGD rate, and electric conductivity of SGD at A4.

Figure 10. Combined data sets for the seepage rates measured by the dye-dilution seepage meter (triangles), and the radon concentration measured by alpha-spectrometer (circles), for the time period when both instruments were running. The water level record (dots) is also shown.

Figure 11. δD vs. δ^{18}O plot for groundwater, seawater and their mixtures (water in monitoring wells and in seepage chambers). GMWL = Global Meteoric Water Line (constructed after Craig, 1961). LMWL = Local Meteoric Water Line (constructed using the IAEA's GNIP (Global Network of Isotopes in Precipitation) data). Notice differences between the GMWL (LMWL) and the regression line for the groundwater-seawater data (correlation coeffiecient r^2 = 0.97, P < 0.0001), which could indicate an influence of seawater-atmospheric water vapor interactions.

Figure 12. (a) Ground conductivity transects at Flamengo Bay as measured during three subsequent days. At each of the stations along the transect (indicated by numbers on the sediment surface), a profile of ground conductivity was recorded, and data was subsequently contoured. Locations of a pronounced change of physical resistance, and hence likely change in sediment type, are marked with orange crosses. The tidal water level at time of recording is shown. Arrows at stations 10, 12 and 15 mark the locations of the manual seepage meters SD1, SD8 and SD2, respectively (see also Fig. 2). The length of the arrows is proportional to the average flux of SGD into each of these seepage meters. In addition, the average salinity of the SGD is given. The grey colour represents basement rock. (b) Shore-parallel bulk ground conductivity and resistivity at Fazenda Beach (conductivity and resistivity are inversely related). The approximate water line at time of recording the data is marked (WL).

Figure 13. An inverse relationship between the observed ^{222}Rn activity concentration of seawater and salinity for Flamengo and Picinguaba Bays (r^2 = 0.93, P = 0.035 and r^2 = 0.92, P = 0.039, respectively). ^{222}Rn activity concentrations in surface seawater in the Flamengo Bay were up to 3 times higher than in the Picinguaba Bay (at similar salinities), that would indicate different sources of groundwater in the bays.

Figure 14. ^{222}Rn versus salinity is plotted to show the rapid loss of Rn from brackish or saline pore waters.

Figure 15. The ln Ra activity as a function of distance offshore for samples collected on the Vitoria Island transect (a) and the Flamengo bay transect (b).

Figure 16. Dependence of the water age on the offshore distance. Samples collected in the bays have ages in the range 2-10 days relative to the water in the seepage meter. Farther offshore from 10 to 25 km the estimated ages are between 7 and 15 days.

Figure 17. (a) Calculated SGD rates based on continuous alpha-spectrometry ^{222}Rn measurements at a fixed location about 300 m off the Oceanography Base together with water level fluctuations. (b) A portion of the same record showing that the SGD peak that did not correspond to a low tide may have been related to a rain event at that time.

Figure 18. Calculated SGD rates based on continuous gamma-spectrometry ^{222}Rn measurements at a fixed location about 15 m off the Oceanography Base together with water level and salinity fluctuations.

Fig. 1.

(a)

● SD6

A4◆ ● SD5
MS4■ □W3B   □W3A

A3◆ ● SD4
        □W2B   □W2A
                                    ★GS

MS3■ ● SD3
Sea   MS5■ ● SD2
            MS2■   Low tide shoreline
        ● WHOI   ● SD1W   A1◆ ● SD1   ● SD1E

Beach
            □W1B   □W1A
    10 m
                    □W0
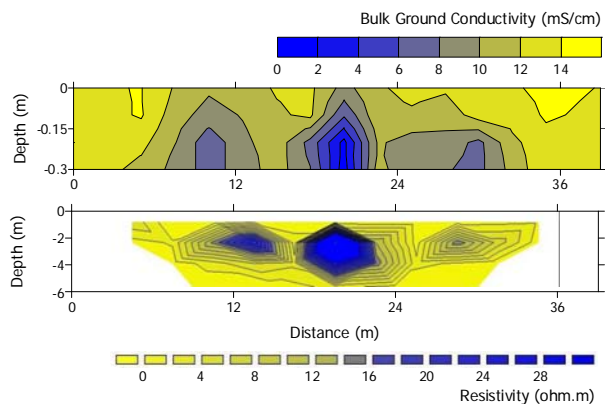
(b)

Fig. 2.

Fig. 3.

Fig. 4.

Figure 5.

Figure 6.

35
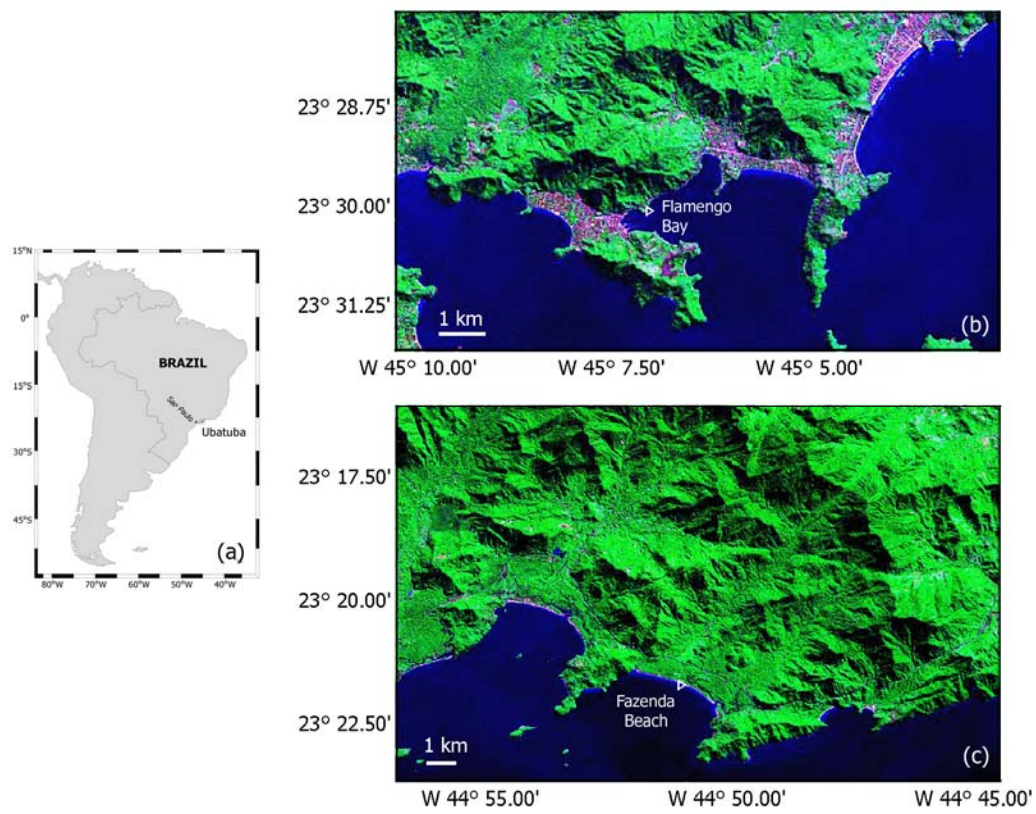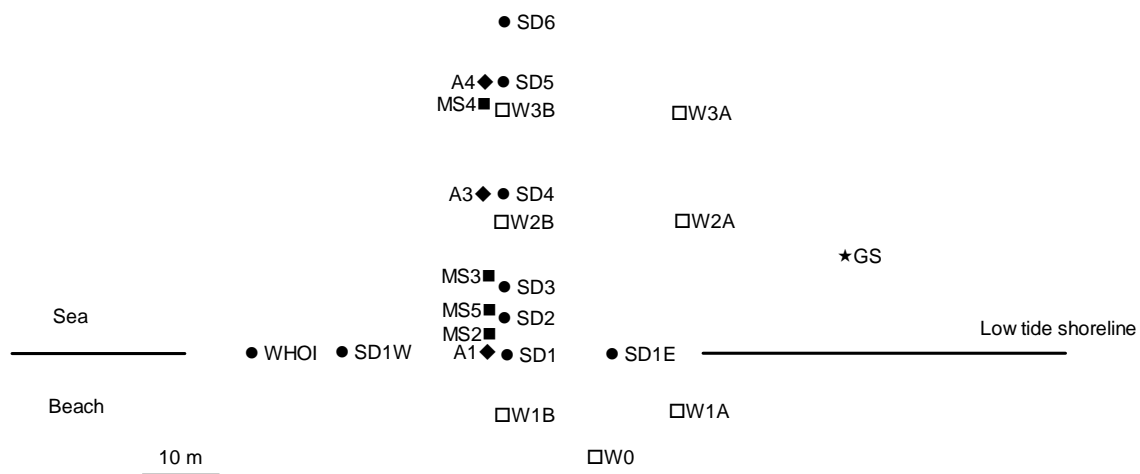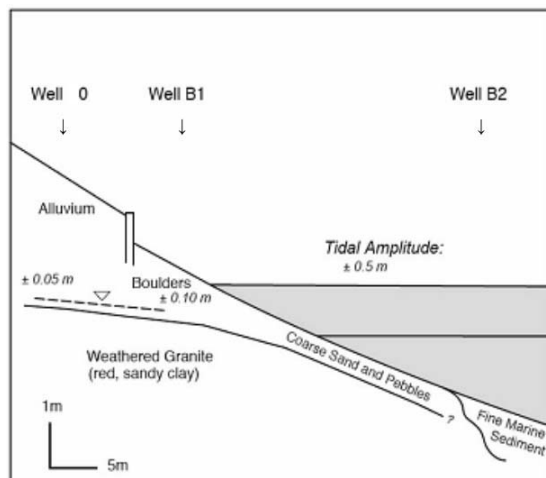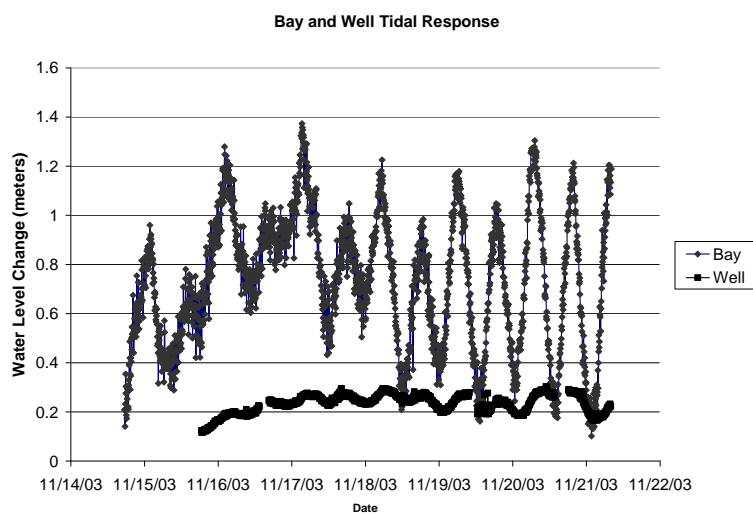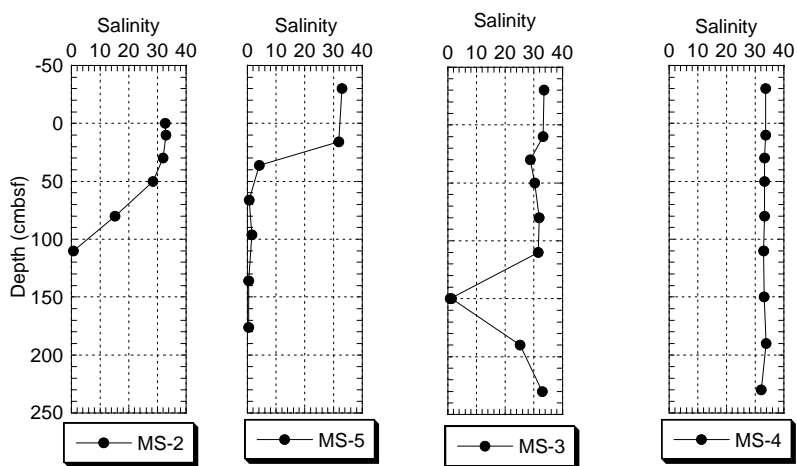
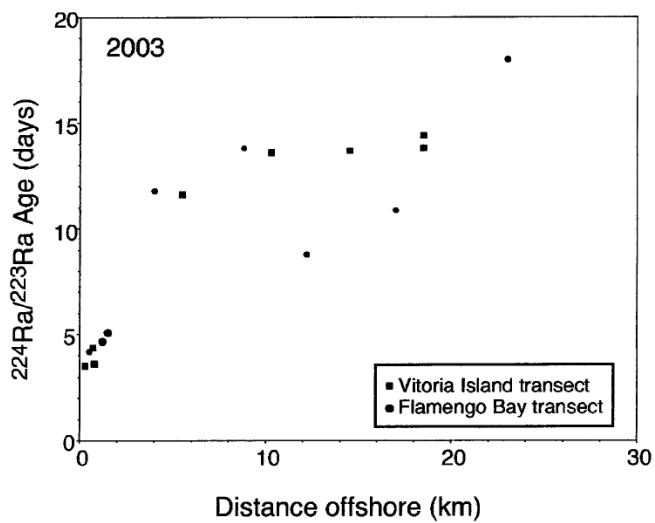Fig. 7.

Fig. 8.

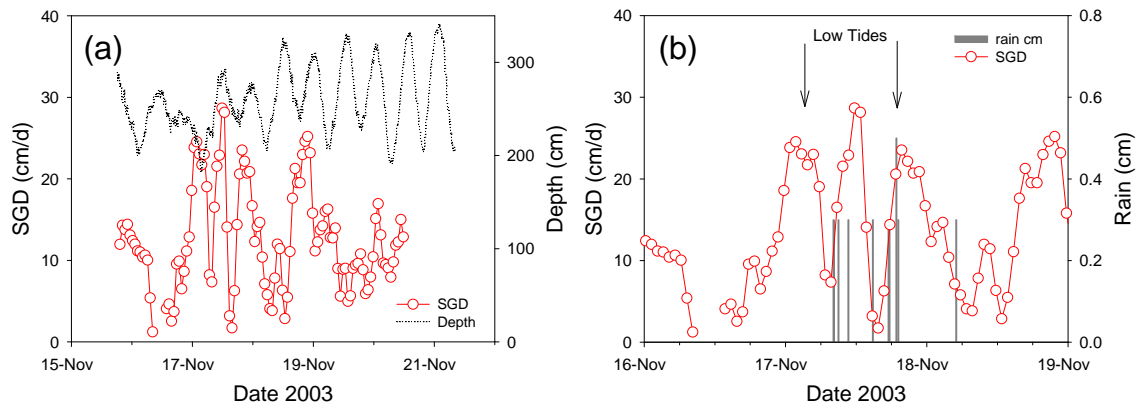Fig. 9.

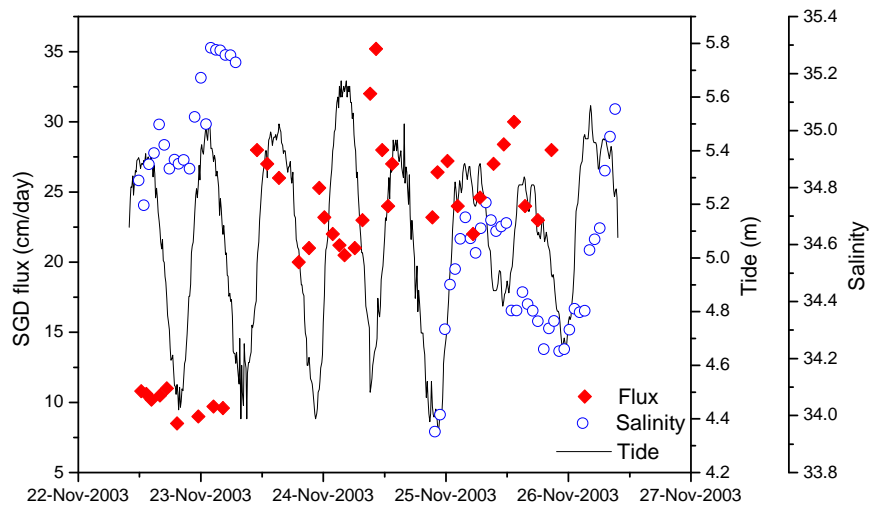Fig. 10

Fig. 11.
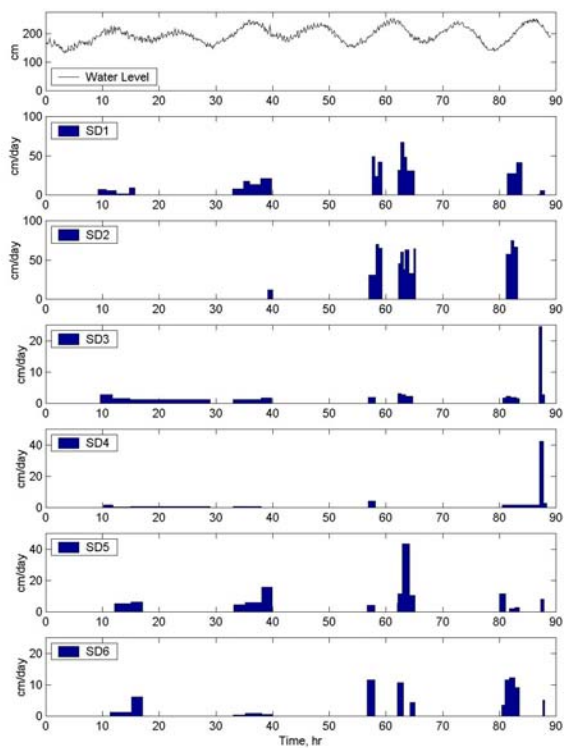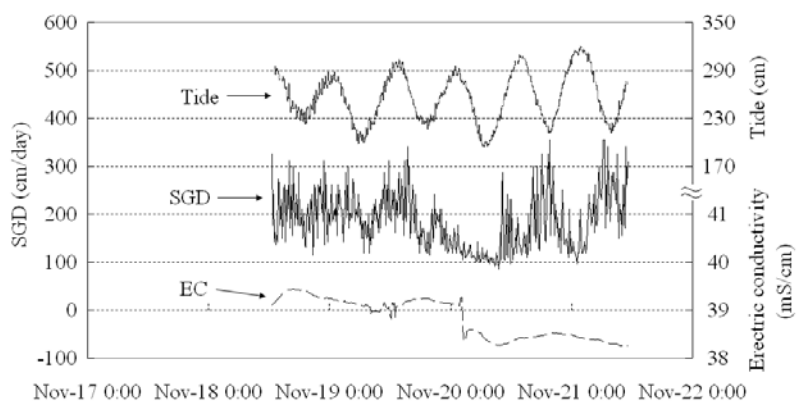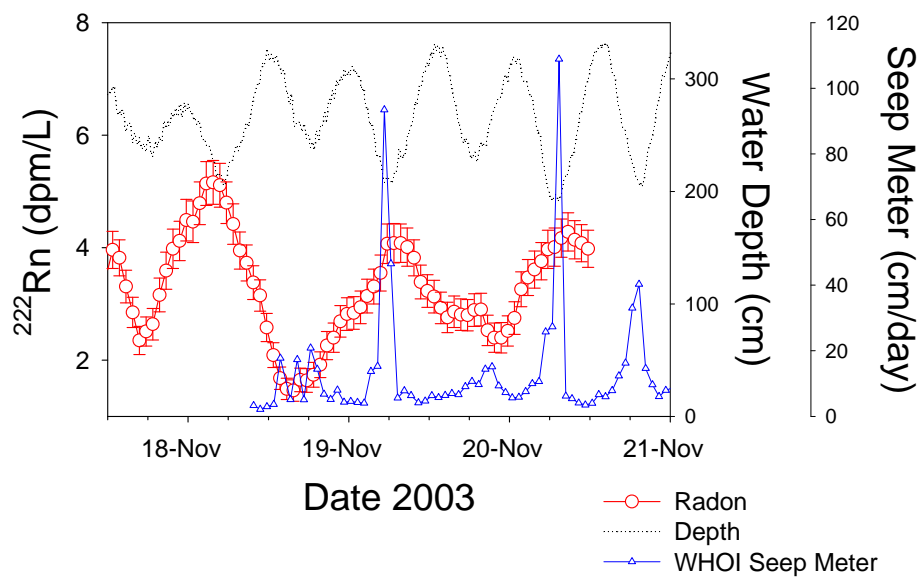
(a)
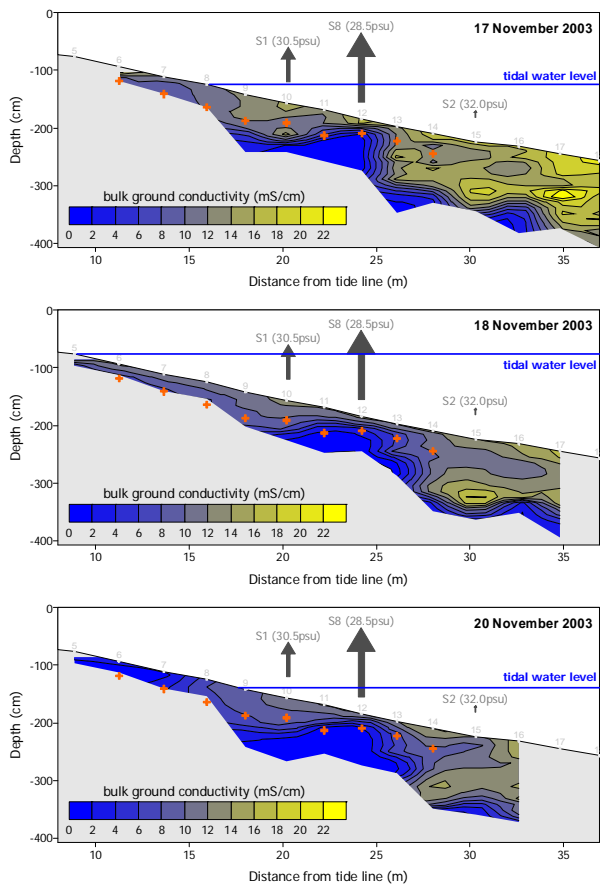
(b)

Fig. 12.
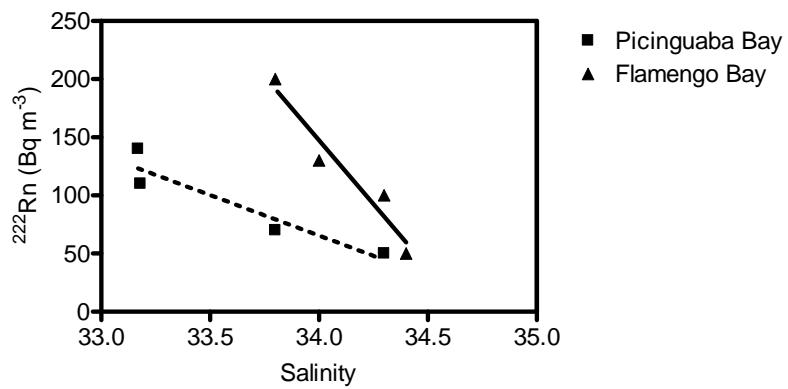
Fig. 13.
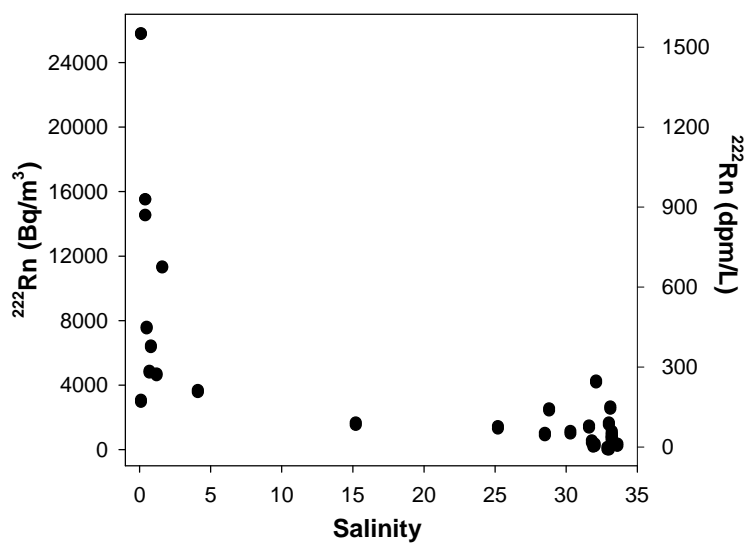
Fig. 14.

Fig. 15.

Fig. 16.

Fig. 17

Fig. 18.